Gene Therapy (2013) **20,** 450–459

www.nature.com/gt

ORIGINAL ARTICLE

Global CNS gene delivery and evasion of anti-AAV-neutralizing antibodies by intrathecal AAV administration in non-human primates

This article has been corrected since online publication and a corrigendum is also printed in this issue

SJ Gray, S Nagabhushan Kalburgi, TJ McCown and R Jude Samulski

Injection of adeno-associated virus (AAV) into the cerebrospinal fluid (CSF) offers a means to achieve widespread transgene delivery to the central nervous system, where the doses can be readily translated from small to large animals. In contrast to studies with other serotypes (AAV2, AAV4 and AAV5) in rodents, we report that a naturally occurring capsid (AAV9) and rationally engineered capsid (AAV2.5) are able to achieve broad transduction throughout the brain and spinal cord parenchyma following a single injection into the CSF (via cisterna magna or lumbar cistern) in non-human primates (NHP). Using either vector at a dose of $\sim 2 \times 10^{12}$ vector genome (vg) per 3–6 kg animal, approximately 2% of the entire brain and spinal cord was transduced, covering all regions of the central nervous system (CNS). AAV9 in particular displayed efficient transduction of spinal cord motor neurons. The peripheral organ biodistribution was highly reduced compared with intravascular delivery, and the presence of circulating anti-AAV-neutralizing antibodies up to a 1:128 titer had no inhibitory effect on CNS gene transfer. Intra-CSF delivery effectively translates from rodents to NHPs, which provides encouragement for the use of this approach in humans to treat motor neuron and lysosomal storage diseases.

Gene Therapy (2013) **20,** 450–459; doi:10.1038/gt.2012.101; published online 10 January 2013

Keywords: AAV; cerebrospinal fluid; brain; spinal cord; non-human primate

INTRODUCTION

Recently, the adeno-associated virus (AAV) serotype 9 capsid was identified as a vector capable of transducing neurons and glia throughout the central nervous system (CNS) following intravenous delivery in adult rodents, cats and non-human primates (NHPs).[1–5] However, the translational feasibility of an intravascular delivery approach for CNS disorders is problematic owing to the high doses required, high biodistribution to peripheral tissues, reduced efficiency for CNS transduction in NHPs and strong inhibition by low levels of circulating anti-AAV9-neutralizing antibodies (NAbs).[3] Intracerebroventricular injection of AAV into the cerebrospinal fluid (CSF) has been used as an alternative approach to transduce the brain, but previously tested AAV serotypes (2, 4 and 5) are not able to penetrate efficiently into the brain parenchyma and transduce neurons without adjuvants such as mannitol; instead, AAV 4 and 5 efficiently transduce the ependymal cells that line the ventricles.[6–8]

Intrathecal injection into the lumbar cistern or injection into the cisterna magna has been used as an alternative approach to deliver AAV to the central and peripheral nervous systems via the CSF. Although these studies have been conducted in rodents with AAV1, AAV2, AAV3, AAV5, AAV6, AAV8 and AAV9, the primary focus has been on spinal cord and/or dorsal root ganglia (DRG) transduction. Conversely, in rodents intrathecal AAV delivery produces only minimal brain transduction.[9–14] For AAV9, transduction of the spinal cord in mice was reportedly efficient but mostly limited to the lower thoracic and lumbar spinal cord.[13] In contrast, when pigs received intrathecal injection of AAV9, the transduction pattern could be diffusely spread across the entire spinal cord if a catheter was used to inject the vector into the CSF directly at the cervical, thoracic and lumbar regions.[15] Interestingly and in contrast to the results in mice, in pigs there was a high degree of brain transduction present regardless of whether the vector was injected diffusely across the spinal cord or just in the lumbar cistern (S Gray, unpublished observation). Very recently, Samaranch *et al.*[5] reported that injection of AAV9 into the cisterna magna of NHPs resulted in widespread brain transduction similar to intravascular delivery. These studies suggest that injection into CSF allows diffuse delivery to large areas of the brain and spinal cord where the doses can be realistically scaled to larger animals and humans.

In this study, we sought to explore the translational potential of intra-CSF delivery of AAV for spinal cord and brain transduction. Based on previously published results[5,13,15,16] and those presented here, AAV2.5 and AAV9 are capable of intraparenchymal neuronal transduction following intra-CSF delivery. AAV9 and AAV2.5 were compared 4 weeks following injection into the cisterna magna in NHPs, and then compared with AAV9 injected into the lumbar intrathecal space. We assessed variables critical for the translation of this approach to humans, including the efficiency of brain and spinal cord transduction, dose response, biodistribution to peripheral organs and evasion of naturally occurring NAbs to the vector.

RESULTS

AAV2.5 is an engineered version of AAV2 that allows transduction of neurons in the brain parenchyma following intra-CSF injection

Following injection of AAV vectors into the ventricles of the brain, natural serotypes of AAV have only been successful at transducing ependymal cells lining the ventricles rather than neurons within

Gene Therapy Center, University of North Carolina at Chapel Hill, Chapel Hill, NC, USA. Correspondence: Dr SJ Gray, Gene Therapy Center, University of North Carolina at Chapel Hill, 7119 Thurston Bowles, Campus Box 7352, Chapel Hill, NC 27599-7352, USA.
E-mail: graysj@email.unc.edu
Received 16 February 2012; revised 23 October 2012; accepted 27 November 2012; published online 10 January 2013

the brain parenchyma.[6] AAV2.5 is a hybrid of AAV2 and AAV1, incorporating six amino acids from AAV1 into the AAV2 capsid.[17] These mutations confer enhanced muscle tropism to AAV2.5, and this capsid was used in a clinical trial for Duchenne's muscular dystrophy.[17] AAV2.5 (10 μl, 6.6×10^{10} vector genome (vg)) was injected into the anterior portion of the right lateral ventricle of adult rats to investigate the potential to transduce neurons following intra-CSF administration. After 2 weeks, the rats were perfused, and tissue sections were taken through the entire rostral–caudal extent of the brain for immunohistochemistry (IHC) and immunofluorescence. As seen in Figure 1, substantial transduction was found in the hypothalamus along the extent of the third ventricle, as well as in the central gray surrounding the Sylvian aqueduct. Furthermore, extensive transduction was found in the subcommissural organ, located within the dorsal third ventricle (Supplementary Figure 1), whereas some green fluorescent protein (GFP)-positive vestibular neurons were found near the fourth ventricle. Importantly, in our previous unpublished studies, this ability to transduce distal structures along the ventricular system was not seen with AAV2, AAV5 or AAV9 (for AAV9, see Supplementary Figure 2).

Injection of AAV9 or AAV2.5 into the cisterna magna of NHPs results in widespread transduction of the entire brain and spinal cord

AAV2.5 showed a unique characteristic that separates it from known naturally occurring AAV capsids, namely, it can cross the ependymal cell barrier and transduce neurons in the CNS following intra-CSF delivery. In our previous studies, AAV9 showed superior ability in transducing the spinal cord following intrathecal delivery in mice and pigs (Supplementary Figure 3 and Snyder *et al*.[13] Federici *et al*.[15]). To compare the potential value of these vectors for gene delivery in human applications, we evaluated AAV2.5 and AAV9 in cynomolgus monkeys, when injected into the CSF of the cisterna magna. Table 1 provides a summary of all the NHPs used in this study. Two NHPs were injected with self-complementary recombinant AAV (scAAV)2.5 (2×10^{12} vg) and two with scAAV9 (1.83×10^{12} vg) in 1.5 ml of phosphate-buffered saline (PBS) containing 5% sorbitol. For direct comparison of the intracisternal versus intrathecal routes, two additional animals were injected via the lumbar cistern with scAAV9 (1.83×10^{12} vg in 1 ml). After 4 weeks, the animals were killed. Serum samples were analyzed for the prevalence of NAbs against the injected capsid, at the time of injection and at the time of sacrifice (Table 2). All animals showed a rise in NAbs of the injected serotype after 4 weeks. After 4 weeks, two animals (101 injected with AAV9 and 104 injected with AAV2.5) produced NAbs against the other serotype, while two animals (102 and 103) did not. The native GFP fluorescence signal was not reliably or readily detectable, thus IHC was used to enhance the signal. GFP expression in the brain, spinal cord and DRG was visualized and quantified by IHC, and vector biodistribution throughout the spinal cord and major peripheral organs was assessed by quantitative polymerase chain reaction (qPCR) (Figure 2). The specificity of the IHC was validated by performing parallel IHC on uninjected NHP samples, on the injected NHP samples without addition of the primary anti-GFP antibody and on injected versus uninjected rat brains (Supplementary Figure 4). The location of the coronal sections portrayed in Figure 2 is shown in Supplementary Figure 5. For the most part, AAV2.5 and AAV9 performed in a roughly equivalent manner throughout the brain and spinal cord, transducing a similar amount of tissue. The biodistribution data favored AAV2.5, which had approximately a 100-fold lower distribution to the spleen compared with AAV9. Both animals injected with AAV2.5 had pre-existing NAbs against the AAV2.5 capsid (1:8 and 1:128); therefore, this could have affected the biodistribution of the vector to peripheral organs.

The two NHPs injected via the lumbar cistern, for the most part, were comparable to those receiving an intracisternal injection. However, unlike the pattern seen following intracisternal injection, the DRG were highly transduced with approximately 15–20% of the area positive for GFP expression.

Table 1. Summary of NHPs in this study

Subject	*Age (years)*	*Weight (kg)*	*Route*	*Capsid*	*Dose ($vg \times 10^{12}$)*	*Volume (ml)*
101	3	2.8	IC	9	1.83	1.5
102	3	2.8	IC	9	1.83	1.5
103	3	2.6	IC	2.5	2.0	1.5
104	3	2.9	IC	2.5	2.0	1.5
303	3	6.3	IT	9	1.83	1.0
304	3	6.9	IT	9	1.83	1.0
201	4–7	4.8	IT	9	1.83	1.0
202	4–7	4.4	IT	9	1.83	1.0
203	4–7	5.1	IT	9	1.83	1.0
204	4–7	4.8	IT	9	1.83	1.0
205	4–7	4.1	IT	9	5.5	1.0
206	4–7	3.5	IT	9	5.5	1.0

Abbreviations: IC, intracisternal; IT, intrathecal; NAb, neutralizing antibody; NHP, non-human primate; vg, vector genomes. .

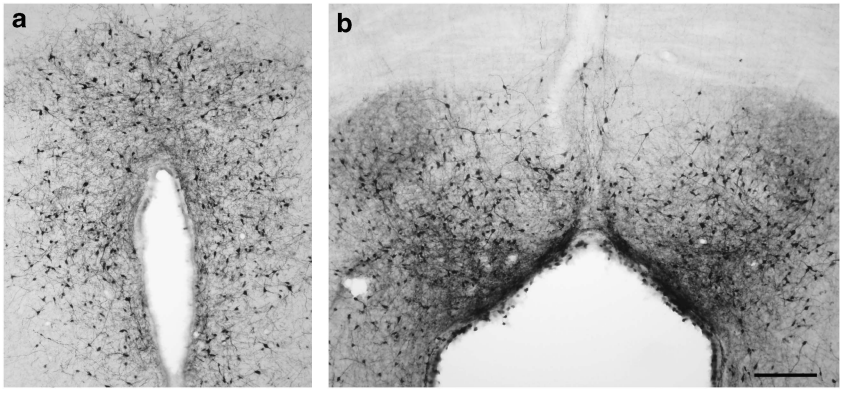

Figure 1. AAV2.5 can cross the ependymal cell barrier and transduce neurons after ventricular administration. AAV2.5/GFP (10 μl, 6.6×10^{10} vg) was injected into the anterior portion of the right lateral ventricle of adult rats, and after 2 weeks, gene expression was assessed by anti-GFP IHC. (**a**) Transduction of cells with neuronal morphology in the hypothalamus along the third ventricle. (**b**) GFP-positive cells with neuronal morphology in the dorsal central gray. Scale bar is 50 μm.

Table 2. NAbs in the serum and CSF, and vector persistence

Subject	*Serum NAb Titer*[a]			*CSF NAb titer*		*CSF*	*CSF*
	Prescreen	*At injection*	*4 Weeks post-inj.*	*At injection*	*4 Weeks post-inj.*	*Vg at 2 h post-injection (per ml)*	*Circulating vg at 2 h*[b]
101	NT	<1:2 (<1:2)	1:2048 (1:2048)	NT	NT	NT	NT
102	NT	1:32 (1:128)	1:1024 (1:4)	NT	NT	NT	NT
103	NT	1:32 (1:128)	<1:2 (1:1024)	NT	NT	NT	NT
104	NT	1:2 (1:8)	1:1024 (>1:2048)	NT	NT	NT	NT
303	<1:2	<1:2	1:256	<1:2	<1:2	NT	NT
304	<1:2	<1:2	>1:2048	<1:2	<1:2	NT	NT
201	1:32	1:32	1:1024	<1:2	<1:2	$<1 \times 10^4$	<0.0001%
202	1:128	1:128	1:1024	<1:2	1:4	3.31×10^5	<0.0001%
203	<1:2	1:4	1:1024	<1:2	<1:2	8.02×10^5	<0.0001%
204	<1:2	<1:2	1:256	<1:2	<1:2	3.30×10^8	0.0007%
205	<1:2	1:8	1:256	<1:2	<1:2	6.96×10^5	<0.0001%
206	<1:2	<1:2	1:64	<1:2	<1:2	$<1 \times 10^4$	<0.0001%

Abbreviations: CSF, cerebrospinal fluid; inj., injection; NAb, neutralizing antibody; NT, not tested (sample not available); vg, vector genome. [a]Values are for NAb titers against AAV9. NAb titers against AAV2.5 are indicated within parentheses when tested. [b]Assuming 12 ml of CSF per animal and an even distribution of AAV particles throughout the entire 12 ml, circulating vg in the CSF was calculated as the percentage of the total vg injected per 12 ml (1.5×10^{11} vg per ml CSF for low dose and 4.6×10^{11} vg per ml CSF for high dose).

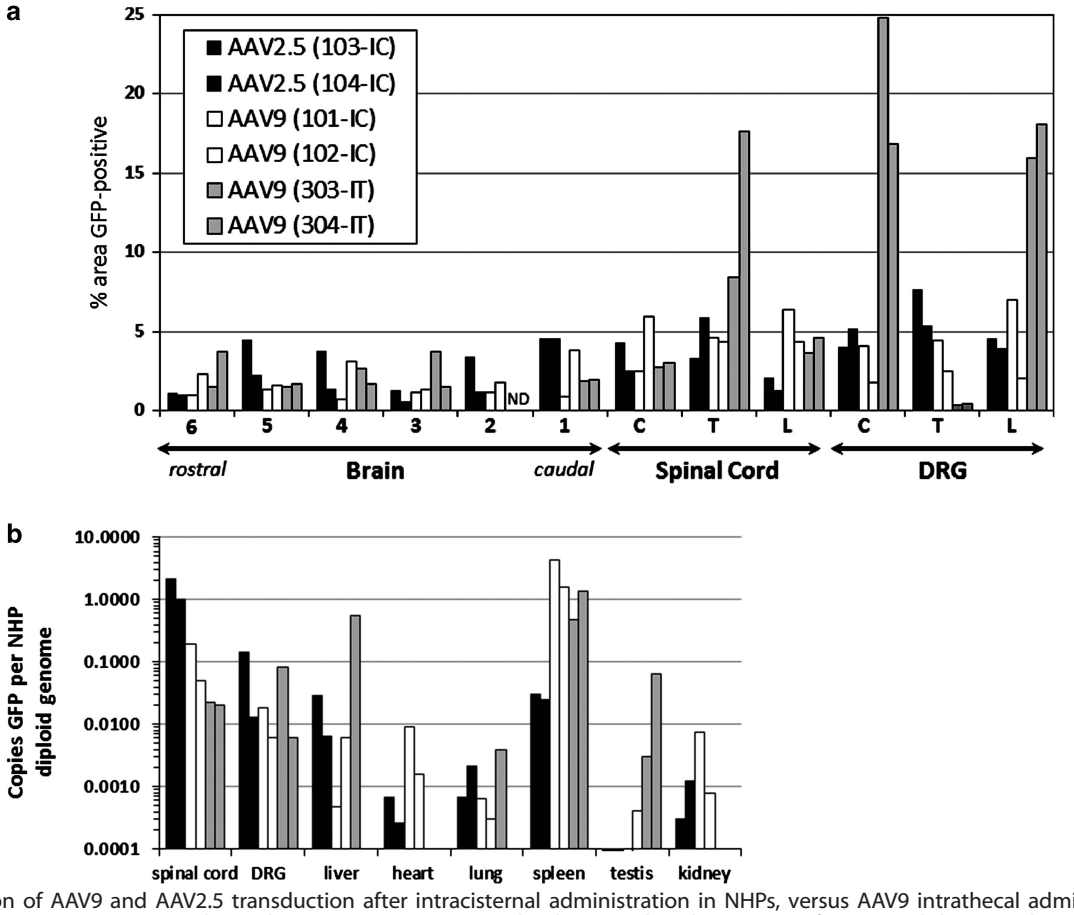

Figure 2. Comparison of AAV9 and AAV2.5 transduction after intracisternal administration in NHPs, versus AAV9 intrathecal administration. scAAV9 or scAAV2.5 vectors were injected into the cisterna magna (IC) or lumbar intrathecal space (IT) of NHPs, and the animals were killed 4 weeks later. (**a**) In all, 5–7 μm sections from the brain, spinal cord and DRG were subjected to IHC against GFP, and then quantified by histomorphometry. For the location of brain samples 1–6, see Supplementary Figure 5. (**b**) Total DNA was purified from the samples, and the copies of GFP relative to the NHP glyceraldehyde-3-phosphate dehydrogenase locus were ascertained by qPCR. C, cervical; T, thoracic; L, lumbar; ND, no data. The legend for both panels is provided in (**a**).

Intrathecal injection of AAV9 avoids pre-existing NAbs and transduces DRG at a higher efficiency than intracisternal injection

Our previous studies in mice by intrathecal injection showed that AAV9 was considerably better at transducing motor neurons than AAV2.5 (Snyder *et al.*[13] and data not shown). For several disease applications (such as spinal muscular atrophy, giant axonal neuropathy and amyotrophic lateral sclerosis), motor neuron transduction is likely to be an important criteria for selecting the

best vector, so we conducted further tests on AAV9 in NHPs to determine the translational feasibility of its use as a gene therapy vector. To test the efficacy of intrathecal gene transfer (relative to intracisternal) in a NHP model, six cynomolgus monkeys were injected with 1.83×10^{12} vg of scAAV9/GFP vectors in 1 ml of $1 \times$ PBS containing 5% sorbitol. To investigate a possible dose–response relationship, an additional two animals were injected with 5.5×10^{12} vg of the same vector, in 1 ml of PBS containing 5% sorbitol. All animals were prescreened for NAbs against AAV9, and two of the 'low-dose' animals were specifically selected because they had naturally occurring NAb titers of 1:32 and 1:128 (Table 2). The animals were killed after 4 weeks. Serum samples were analyzed for prevalence of NAbs against the injected capsid at the time of injection and at the time of sacrifice. Two of the animals had tested negative for NAbs in the prescreen 2 months before injection, but had (1:4 and 1:8) titers of NAbs at the time of injection. CSF was collected from the cisterna magna at the time of injection, 2 h post-injection and at the time of sacrifice to check for neutralizing factors in the CSF before and after injection, as well as to assess the persistence of the vector at 2 h post-injection (Table 2). We found that at pre- and post-injection time points, the CSF did not contain any factors that inhibited AAV transduction, except in one animal at the 4-week time point (1:4 dilution). This animal (202) had the highest pre-existing NAb titer (1:128) and an even higher titer (1:1024) at 4 weeks following injection. NHP 202 had a low but detectable amount of NHP DNA in the 4-week CSF sample, indicating some blood contamination of the collected CSF, which could explain the presence of NAbs in the CSF (see Supplementary Table 1). All animals examined had virtually no vector remaining in circulation in the CSF at 2 h post-injection, at least in the cisterna magna (Table 2).

GFP expression in the brain, spinal cord and DRG was visualized and quantified by IHC, and vector biodistribution throughout the brain, spinal cord, DRG and major peripheral organs was assessed by qPCR. For most of the animals (three low-dose NAb +, one low-dose NAb −, two high-dose), IHC was performed on the liver and spleen to assess vector expression in these peripheral organs. To compare broadly how the experimental variables affected gene expression in an unbiased and quantitative manner, anti-GFP IHC was carried out on 5–7 μm sections from all samples and subjected to automated morphometric analysis to assess gene expression throughout the brain, spinal cord, DRG, optic nerve, liver and spleen (Figure 3a and Supplementary Table 2, locations of coronal sections shown in Supplementary Figure 6). Both the gray and white matter showed expression of GFP that was not evident in sections prepared in parallel without the primary anti-GFP antibody or on naïve tissue (Supplementary Figure 4). The percent area of each slice that is GFP positive does not necessarily correlate to the percentage of cells transduced. In all, we found no difference in the distribution of CNS or peripheral organ GFP expression between any groups, regardless of the presence of anti-AAV9 NAbs or the vector dose. The distribution of GFP expression was fairly even across the entire brain and spinal cord, with an average value of approximately 2% of the area positive for GFP in any given region of the CNS. The vector DNA biodistribution mostly followed the same pattern as GFP expression, with a few notable exceptions (Figure 3b). The spinal cord had more vector genomes than the brain, and these levels were comparable to the DRG, except in the high-dose group where the DRG were at least 10-fold higher. When compared with intravascular delivery of AAV9,[3] intrathecal delivery resulted in a much lower proportion of vector genomes in peripheral organs compared with the CNS. Although high levels of vector genomes were detected in the liver, the presence of vector genomes did not correlate with a large portion of the liver being positive for GFP expression. Similarly, although over 50 times more vector genomes were detected in the spleen than the brain, only approximately 2–5% of the spleen was positive for GFP expression. Interestingly, the presence of pre-existing AAV9 NAbs did not correlate with lower biodistribution to peripheral organs.

To illustrate how the 'percent of area GFP positive' correlates to the percentage of positive cells, sample images of those used for the quantitative IHC portrayed in Figure 3a are provided in Figure 4 (spinal cord, DRG, liver and spleen) and Figure 5 (brain). Manual counting of GFP-positive versus -negative cells was carried out across animals 201–206, focusing on specific brain and spinal cord structures, and this information is provided in Table 3 with representative photographs of each region provided in Supplementary Figure 7. Although there were modest differences in the overall transduction efficiency of specific brain structures, all areas were transduced regardless of their proximity to the CSF.

In the ventral horn of the spinal cord, an abundance of large diameter (25–50 μm) cells were GFP-positive, indicating efficient transduction of motor neurons. This is confirmed by the colocalization of GFP and ChAT seen in Supplementary Figure 8. Consistent with previous reports,[5] we observed transduction of both neurons and astrocytes throughout the brain and spinal cord (Supplementary Figures 9 and 10). A similar degree of spread throughout the brain parenchyma, along with transduction of neurons and glia, was observed in mice (Supplementary Figure 3). Interestingly, in some sections, we captured part of the choroid plexus within the lateral ventricle (Figure 6). The choroid plexus was very strongly GFP positive, in stark contrast to the lack of GFP expression in the ependymal cells that line the ventricles.

DISCUSSION

Based on our results, we conclude that intra-CSF administration of AAV9 or AAV2.5 vectors (via lumbar cistern or cisterna magna) offers a viable, translational option for global CNS gene delivery. Importantly, these studies appear to have a marked improvement in overcoming previously identified translational barriers, such as inhibition by pre-existing NAbs, high peripheral organ biodistribution, reduced efficiency of CNS transduction in NHPs compared with rodents and high dosage requirement[3]). It should be noted, however, that intrathecal administration, especially for AAV9, did not completely restrict the vector within the CNS. The additional success of AAV2.5 in this approach also demonstrates the ability to engineer rationally improved functionality into the AAV capsid for novel clinical applications. If very high titers of NAbs can inhibit the transduction of AAV9 after intra-CSF delivery, as the results of Samaranch *et al.*[5] suggest, the availability of two distinct AAV serotypes capable of widespread CNS transduction would allow treatment of patients with high levels of NAbs against one of these serotypes (but not both). Two out of four animals showed a lack of NAb cross-presentation between AAV2.5 and AAV9 (Table 2), suggesting the possibility of a second administration of vector in some populations if the serotype capsid was switched on the second administration.

Evasion of anti-AAV NAbs is an important consideration for any translational approach, as an estimated 33.5% of the human population are seropositive for AAV9.[18] In this study and others, we have screened a total of 35 randomly selected naïve NHPs for anti-AAV9 NAbs, and the highest titer detected was 1:128. Although Samaranch *et al.*[5] reported that anti-AAV9 serum NAb titers $\geqslant$1:200 inhibited CNS gene transfer when AAV9 was injected via the cisterna magna, in the present studies we found that anti-AAV serum NAb titers up to 1:128 had no inhibitory effect on successful CNS gene transfer. No inhibitory factors were identified in the CSF before vector delivery or at 4 weeks post-injection, even when post-injection serum NAb titers rose as high as 1:2048. Previously, we found that a 1:4 NAb titer was sufficient to inhibit completely AAV9 transduction of the CNS and peripheral organs if an intravascular route of administration was used.[3] Although the results of Samaranch *et al.*[5] indicate that high serum NAb titers can negatively influence intra-CSF gene transfer, our

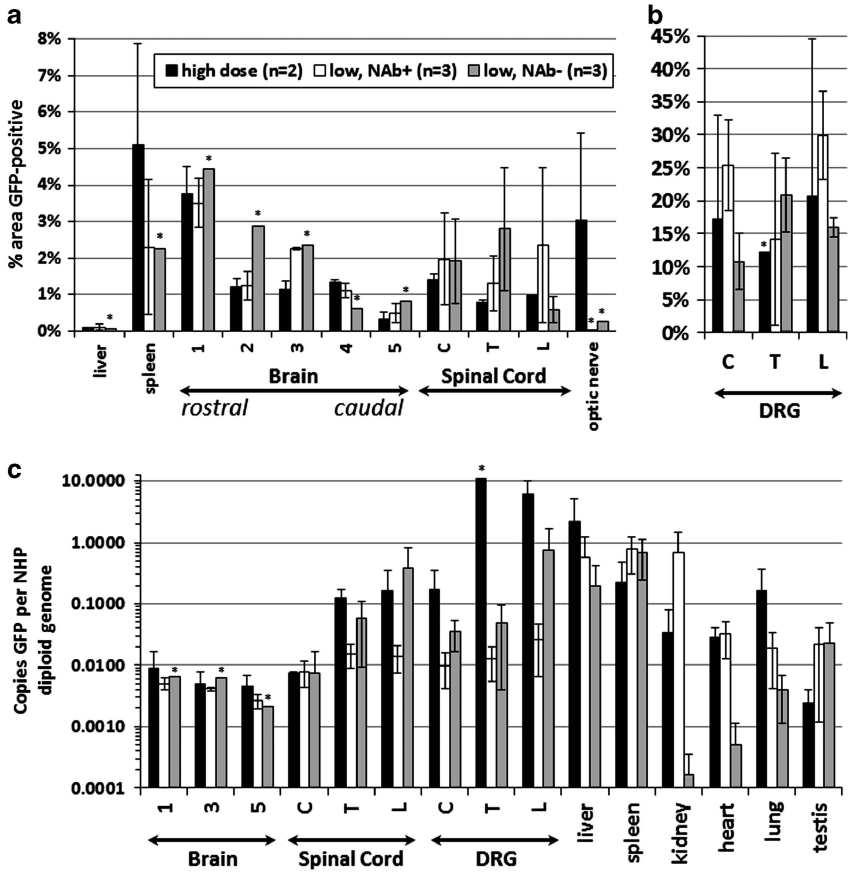

Figure 3. Intrathecal AAV9 injection in NHPs provides widespread CNS transduction with reduced peripheral biodistribution and evasion of NAbs. NHPs received a single intrathecal injection of 1.83×10^{12} vg (low-dose) or 5.5×10^{12} vg (high-dose) scAAV9/CBh-GFP. After 4 weeks, the animals were killed and the indicated samples from the CNS and peripheral organs were processed. (**a** and **b**) Samples were sectioned at 5–7 μm and subjected to IHC against GFP with histomorphometric quantification of GFP expression. (**c**) Total DNA was purified from the samples, and the copies of GFP relative to the NHP glyceraldehyde-3-phosphate dehydrogenase (GAPDH) locus were ascertained by qPCR. All brain measurements are the average of all quadrants per block analyzed. For the location of brain samples 1–5 and individual data points, see Supplementary Figure 6 and Supplementary Table 2. Brain IHC for animals 303 and 304 examined slightly different brain areas, thus these data are portrayed only in Figure 2. C, cervical; T, thoracic; L, lumbar. Asterisks indicate tissues where a sample from only one animal was tested. NAb + = NAb titer >1:2 and NAb − = NAb titer <1:2. All error bars are s.e.m. The legend for all panels is provided in (**a**).

results clearly show that lower NAb titers (that would block intravascular gene delivery) are well tolerated. Moreover, our limited survey of pre-existing NAb levels in NHP would suggest that the presence of naturally occurring NAbs at levels inhibitory to intra-CSF vector administration would be rare. The methods of titering the NAbs were different in these studies, so we cannot comment on what level of NAb would be inhibitory in relation to our study.

This NHP study yielded some notable differences compared with previous intrathecal AAV9 delivery studies in mice and pigs.[13,15] In pigs, the vector distribution was mostly limited to the lumbar spinal cord, unless a catheter was manipulated to physically distribute the vector to the cervical and thoracic regions. However, in NHPs, a single bolus injection at the lumbar region provided a relatively even level of transduction to the entire spinal cord and brain. Although no clear explanation exists, differences in size, anatomy and species must be considered. For example, unlike humans and monkeys, the pig epidural space contains fatty deposits that may restrict CSF flow.[19] In pigs, the biodistribution to peripheral organs was barely detectable, whereas in NHPs the vector was detected in the liver and spleen at levels that equaled or exceeded levels seen in the CNS. Also, the CSF and CNS volumes across species and age does not always correlate with overall body size, so comparing 'equivalent' doses across species becomes a matter of which metric is used for scaling. In our case, we utilized CSF volume as our comparative metric, assuming equivalent CSF volumes of 0.035 ml in mice, 0.09 ml in rats, 20 ml in pigs, 12–15 ml in NHPs and 140 ml in humans.[20–22] In this case, the high dose in the referenced pig study ($\sim 1.5 \times 10^{11}$ vg per ml of CSF)[15] is equivalent to the low dose used in this study in NHPs ($\sim 1.5 \times 10^{11}$ vg per ml of CSF). Again, it is unclear whether the increased peripheral biodistribution in NHPs compared with pigs is the result of physiological/anatomical differences, differential receptor biology and binding kinetics of AAV9, or differences in the injection protocol that could have led to vector leakage. Previous studies have indicated that intrathecal delivery in mice may restrict the vector to the lower spinal cord, although these studies were carried out with a lower AAV titer.[23] However, our present results show a similarity in the CNS and peripheral biodistribution between mice and NHPs receiving intrathecal injections at equivalent doses (scaled by CSF volume), including transduction throughout the brain (Supplementary Figure 3). The roughly equivalent translation of the intrathecal approach between mice and NHPs is in contrast to an intravenous approach, which works considerably better in mice than NHPs.[3]

A confusing observation from our rodent studies was the lack of widespread transduction following intraventricular injection of

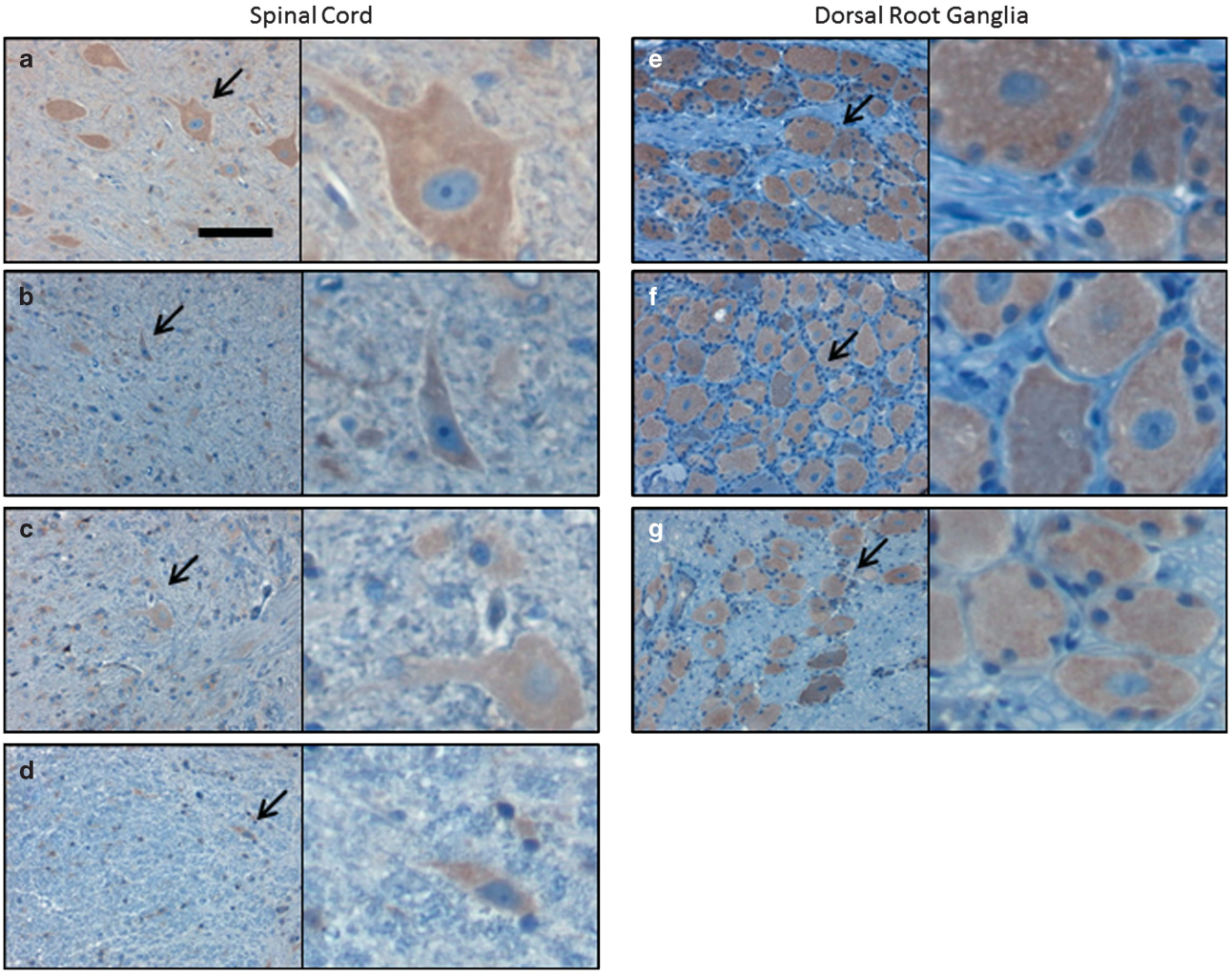

Figure 4. The NHP spinal cord and DRG are efficiently transduced following intrathecal AAV9 vector administration. At 4 weeks following intrathecal injection of scAAV9/CBh-GFP vector, 5–7 μm sections from the spinal cord and DRG were subjected to IHC against GFP. Shown are sample images from those used for histomorphetric quantitation in Figure 3, and more information is available in Supplementary Figure 6 and Supplementary Table 2. These images are from NHP 203 and the specific areas are as follows, with spinal cord in panels a–d and DRG in panels e–g: (**a**) cervical, ventral gray matter; (**b**) thoracic, ventral white matter; (**c**) lumbar, dorsal gray matter; (**d**) lumbar, dorsal white matter; (**e**) cervical; (**f**) thoracic; and (**g**) lumbar. For each panel, the right image is a 4 × enlargement of the area indicated by an arrow, and the total width of the right field is 55 μm. Slides are counterstained with cresyl violet (blue) to show nuclei, and brown (DAB) indicates GFP expression. Scale bar in (**a**) is the same for all panels and is 55 μm.

vector, whereas injections into the lumbar cistern produced widespread CNS transduction (Supplementary Figures 2 and 3). As CSF flows in the direction from the lateral ventricles to the lumbar cistern, it was not clear why the lateral ventricle injection did not work. A possible explanation is that AAV9 has a very high affinity for the ependymal cells of the choroid plexus, supported by the very strong transduction of this structure that we observed in the NHPs (Figure 6). Injection into the lumbar cistern allows the vector to circulate in the CSF before contacting the choroid plexus, whereas injection into the ventricles would concentrate the AAV9 vector around those cells from the moment of injection. Transduction of the choroid plexus itself could be beneficial in certain therapeutic applications, as these cells would be ideal 'factories' to secrete factors into the CSF. However, the turnover of these cells would likely undermine long-term persistent transgene expression from the choroid plexus, as AAV genomes do not normally persist in dividing cell populations.

Several factors should be considered to achieve efficient, global CNS gene transfer with AAV9. First, the present studies exclusively employed self-complementary AAV vectors, which have at least a 20-fold advantage over traditional single-stranded vectors in terms of transduction efficiency.[3,24,25] As these studies utilized self-complementary AAV vectors, this would limit the entire gene expression cassette (minus inverted terminal repeats) to approximately 2.1 kb. Larger gene cassettes (up to approximately 4.6 kb) could be packaged in single-stranded vectors, but a larger dose would likely be required to compensate for the lower efficiency of traditional single-stranded AAV vectors. In this study, we used a hyperosmolar buffer composed of PBS containing 5% sorbitol, which is a common AAV storage buffer to prevent vector aggregation and possible precipitation at higher concentrations. The volume of the injection was low (1 ml compared with a normal CSF volume of ~12–15 ml in an NHP), thus only a small and transient change in the overall CSF osmolarity would be expected, but we cannot exclude the possibility that this affected the biodistribution in some way. In our previous study on intravascular AAV9 delivery to the CNS in NHPs, we used a dose of $\sim 9 \times 10^{12}$ vg per kg ($\sim 3–4 \times 10^{13}$ per animal).[3] Our present intra-CSF study used a low dose of 1.8×10^{12} vg (approximately 6×10^{11} vg per kg or 1.5×10^{11} vg per ml CSF) per animal and a

threefold higher dose of 5.5×10^{12} vg per animal. Interestingly, we did not see an increase in transduction efficiency between our low- and high-dose intrathecal groups, which may suggest that our low dose is already a saturating dose for AAV9 under the present study parameters. However, with the low number of high-dose animals ($n = 2$), we cannot draw any firm conclusions. It is entirely possible that a lower dose could provide a similar level of transduction, but there remains the need for new vector development to increase the transduction efficiency beyond the 'saturated' capabilities of AAV9. Samaranch *et al.*[5] concluded that intravascular and intracisternal AAV9 transduction was equivalent,[5] but they were using a higher intravascular dose of 3×10^{13} vg per kg, and if the intra-CSF dose (1.8×10^{13} vg per kg) was already past saturated levels, then their study may have missed the transduction advantage that intra-CSF delivery provides at lower doses. Based on our results, we conclude that AAV9 intrathecal delivery is superior to intravascular delivery to achieve global CNS transduction, both in terms of transduction efficiency and lack of translational barriers.

In summary, AAV9 and AAV2.5 can be delivered in a NHP by intra-CSF injection to deliver globally a transgene to the entire CNS. Intrathecal injections are routine non-surgical procedures that are often carried out in an outpatient setting with minimal risk. This approach has strong translational implications for lysosomal storage diseases, or any other approach in which a secreted gene product is utilized. The efficiency of spinal cord transduction would also suggest feasible applications for motor neuron diseases, such as spinal muscular atrophy, giant axonal neuropathy and amyotrophic lateral sclerosis.

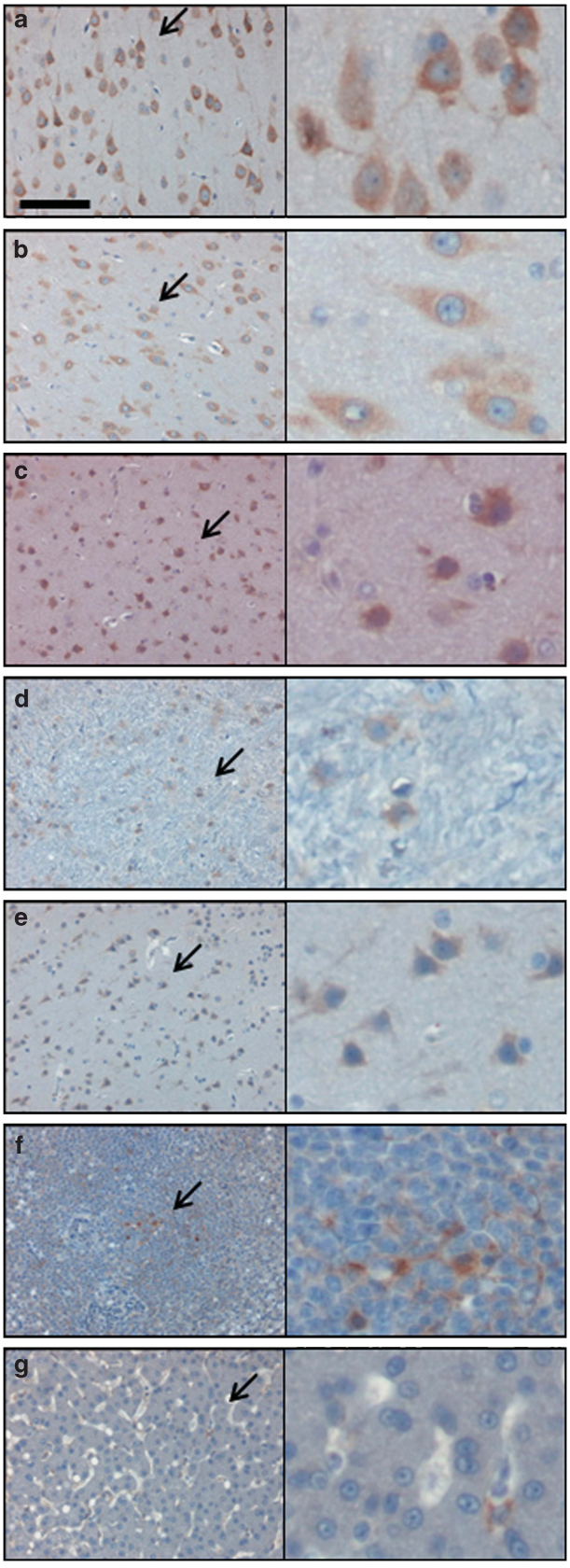

Figure 5. The NHP brain is transduced following intrathecal AAV9 vector administration. At 4 weeks following intrathecal injection of scAAV9/CBh-GFP vector, 5–7 μm sections from the spinal cord and DRG were subjected to IHC against GFP. Shown are sample images from those used for histomorphetric quantitation in Figure 3a, and more information is available in Supplementary Figure 6 and Supplementary Table 2. These images are from NHP 203 brain and the specific areas are as follows: (**a**) brain region 1C; (**b**) brain region 2B; (**c**) brain region 3C; (**d**) brain region 4; (**e**) brain region 5B; (**f**) spleen; and (**g**) liver. For each panel, the right image is a 4× enlargement of the area indicated by an arrow, and the total width of the right field is 55 μm. Slides are counterstained with cresyl violet (blue) to show nuclei, and brown (DAB) indicates GFP expression. Scale bar in (**a**) is the same for all panels and is 55 μm.

MATERIALS AND METHODS

Virus preparation

Recombinant AAV vectors were generated using HEK293 cells grown in serum-free suspension conditions in shaker flasks, using proprietary methods developed at the UNC Gene Therapy Center Vector Core facility (Chapel Hill, NC, USA). In brief, the suspension HEK293 cells were transfected using polyethyleneimine (Polysciences Inc., Warrington, PA, USA) with the following helper plasmids (pGSK2/9 or pXR2.5, and pXX6–80; Xiao *et al.*[26]) plus the inverted terminal repeat-flanked transgene construct pTRS-KS-CBh-EGFP (referred to throughout this manuscript as GFP),[16] to generate self-complementary AAV vectors. At 48 h post-transfection, cell cultures were centrifuged and supernatant was discarded. The cells were resuspended and lysed through sonication as described.[27] DNase (550 U) was added to the lysate and incubated at 37 °C for 45 min, followed by centrifugation at 9400 *g* to pellet the cell debris and the clarified lysate was loaded onto a modified discontinuous iodixanol gradient followed by column chromatography. Purified vectors were dialyzed in 1 × PBS containing 5% D-sorbitol. Titer was obtained by dot blot.[27]

Rodent studies

Animals were maintained in a 12 h light–dark cycle and had free access to food and water. All care and procedures were in accordance with the Guide for the Care and Use of Laboratory Animals (DHHS Publication No. (NIH) 85-23), and all procedures received prior approval by the University of North Carolina Institutional Animal Care and Usage Committee.

Table 3. GFP-positive cells in various brain and spinal cord regions

Brain area	*NHP 201*	*NHP 202*	*NHP 203*	*NHP 204*	*NHP 205*	*NHP 206*	*Average*	*Standard deviation*
1A caudate	63.0	56.5	52.7	51.7	50.5	50.6	54.2	4.9
1A putamen	54.7	52.2	51.2	50.5	50.3	50.1	51.5	1.8
1A thalamus	64.0	45.1	58.6	43.5	57.4	43.1	51.9	9.1
1B amygdala	58.7	58.9	49.9	54.1	48.0	53.0	53.8	4.5
1B lateral geniculate nucleus	41.7	59.7	41.1	59.2	41.0	59.1	50.3	9.9
1B lateral globus pallidus	62.7	50.8	55.2	65.4	45.8	58.8	56.5	7.4
2A corpus callusum	63.4	60.0	51.4	53.9	48.8	52.5	55.0	5.6
2A motor cortex	62.5	57.1	52.2	52.2	50.0	51.1	54.2	4.7
2B hippocampus	50.6	61.8	45.0	57.9	43.7	57.0	52.7	7.4
2B hypothalamus	56.3	69.7	44.7	60.9	42.3	59.0	55.5	10.3
2B thalamus	37.9	54.2	41.1	56.9	42.0	57.5	48.3	8.9
3B midbrain	40.6	65.4	38.3	63.0	37.8	62.5	51.3	13.6
5 Cerebellum	65.5	65.9	49.8	56.9	46.7	54.9	56.6	7.9
5 Pons	55.6	48.5	53.4	47.6	52.8	47.4	50.9	3.5
Cervical spinal cord	45.1	26.2	63.2	29.3	68.3	30.0	43.7	18.4
Thoracic spinal cord	25.0	38.0	39.7	48.9	44.8	52.2	41.4	9.7
Lumbar spinal cord	74.6	52.6	58.6	100	37.0	73.0	66.0	21.7

Abbreviations: GFP, green fluorescent protein; IHC, immunohistochemistry; NHP, non-human primates. GFP-positive cells were manually counted in 5–7 μm sections after anti-GFP IHC, and expressed as a percentage of the total number of cresyl violet-stained nuclei in the same section.

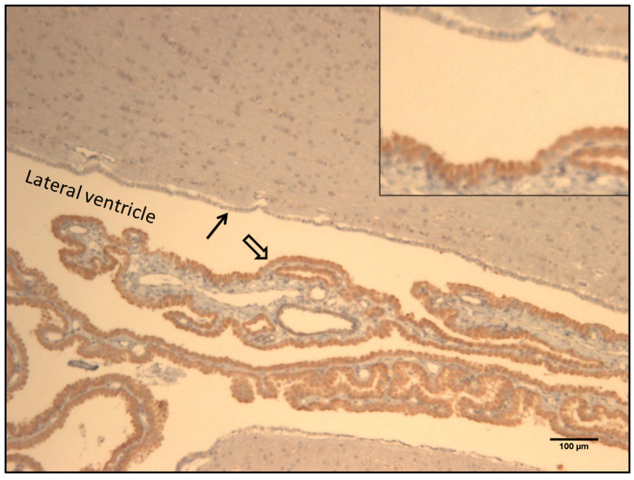

Figure 6. AAV9 strongly transduces the choroid plexus after intrathecal administration in NHPs. At 4 weeks following intrathecal injection of scAAV9/CBh-GFP vector, 5–7 μm sections were collected and subjected to IHC against GFP. The image is from NHP no. 206, block 2A (see Supplementary Figure 6), with the lateral ventricle and surrounding parenchyma shown. Dense GFP staining is observed in virtually all of the ependymal cells of the choroid plexus (open arrow), no GFP seen in the ependymal cells lining the ventricles (closed arrow) and light GFP staining is seen in some cells within the surrounding parenchyma. The scale bar is 100 μm, and the inset is a × 2 magnification of the area highlighted by the arrows.

For AAV infusions into the brain, rats (pathogen-free male Sprague–Dawley rats obtained from Charles Rivers, Burlington, MA, USA; $N = 3$) first were anesthetized with a 50 mg kg intraperitoneal dose of pentobarbital and placed into a stereotaxic frame. Using a 32-gauge stainless-steel injector and a Sage infusion pump, the rats received 10 μl of single-stranded AAV 2.5 (6.6×10^{10} vg) over 10 min into the right lateral ventricle (0.6 mm anterior to Bregma, 1.2 mm lateral, 4.0 mm vertical, according to the atlas of Paxinos and Watson[28]). The injector was left in place for 3 min post-infusion to allow diffusion from the injectors. In all cases, the incision was sutured, and the animals were allowed to recover for 14 days. At 2 weeks after ventricular AAV administration, the rats received an overdose of pentobarbital (100 mg kg pentobarbital, intraperitoneally) and were perfused transcardially with ice-cold 100 mM sodium PBS (pH 7.4), followed by 4% paraformaldehyde in phosphate buffer (pH 7.4).

Mouse intrathecal injections were given in 8- to 12-week-old female BALB/c mice weighing approximately 20 g, purchased from Jackson Laboratory (Bar Harbor, ME, USA). A measure of 5 μl of the vector solution (8.75×10^9 or 1×10^{10} totalvg per mouse) was injected into the intrathecal space of the lower lumbar cord in a non-sedated mouse, as described in Hylden and Wilcox.[29] For intrathecal delivery, scAAV9 vector was prepared in a vehicle solution containing 10–12.5% lidocaine-HCl (MPI Biomedicals, Solon, OH, USA) in 1 × PBS + 3.75% sorbitol. Needle penetration into the intrathecal space was indicated by a tail flick, thereafter successful injections were confirmed by transient (10–15 min) bilateral paralysis of the hindlimbs from the lidocaine.[30] Animals that did not receive a successful injection were removed from the study. Mixing AAV2 with lidocaine did not affect its transduction of HEK293 cells, and injecting AAV9 into mice (intrathecally) without lidocaine did not alter the transduction pattern (data not shown). At termination, the mice were transcardially perfused with PBS containing 1 U ml heparin (Abraxis Pharmaceutic Products, Shaumburn, IL, USA).

qPCR and biodistribution

qPCR was used for vector biodistribution studies. Tissue DNA was purified and quantitated as described.[3] Data are reported as the number of double-stranded GFP DNA molecules per two copies of the monkey glyceraldehyde-3-phosphate dehydrogenase (GAPDH) locus, or in other words the number of vector DNA copies per diploid NHP genome.

Immunolabeling and imaging of samples (rodent samples)

After 48 h of fixation in PBS with 4% paraformaldehyde, tissue samples were sectioned at 40 μm using a Leica vibrating microtome at room temperature. To enhance the signal observed with GFP, IHC was performed. Samples were incubated for 1 h at room temperature in blocking solution (10% goat serum, 0.1% Triton X-100, 1 × PBS), and then incubated 48–72 h at 4 °C in primary antibody solution (3% goat serum, 0.1% Triton X-100, 1 × PBS, rabbit anti-GFP (1:500; Millipore, Billerica, MA, USA; no. AB3080)). After washing three times in 1 × PBS, secondary amplification was performed using a VectaStain ABC Elite Kit (Vector Labs, Burlingame, CA, USA; no. PK-6101) with 3,3′-diaminobenzidine tetrachloride (DAB; Polysciences Inc.; no. 04008) substrate and nickel–cobalt intensification of the reaction product.

For immunofluorescence (Supplementary Figure 1), sections were incubated with a monoclonal antibody to Nestin (1:1000; Chemicon, Temecula, CA, USA). Following incubation for 48 h, the sections were rinsed with PBS and blocked again for 30 min at room temperature in PBS containing 10% goat serum. Sections were then incubated for 45 min at 4 °C with Alexa Fluor 594-conjugated goat anti-mouse immunoglobulin G (1:500; Invitrogen, Carlsbad, CA, USA) in PBS containing 3% goat serum. Rinsed sections were mounted and fluorescence was visualized by confocal microscopy.

Microscopy

DAB-processed brain sections were digitized using a Scan-Scope slide scanner (Aperio Technologies, Vista, CA, USA). Virtual slides were viewed

using ImageScope software package (v. 10.0; Aperio Technologies), and images were generated using the same software. For immunofluorescence studies, colocalization with native GFP fluorescence was determined from a minimum of five consecutive steps in a *Z*-series taken at 1-μm intervals through the section of interest using a × 40 objective.

NHP studies

Animals, surgeries, necropsy and tissue processing (performed by MPI Research). NHP studies were conducted on a contractual basis by MPI Research (Mattawan, MI, USA), in accordance with NIH guidelines and approved by their Institutional Animal Care and Use Committee. Male cynomolgus macaques (*Macaca fascicularis*) were used, with weights and ages provided in Table 1, and all study animals received standard housing and care. For injections into the cisterna magna, the animals were sedated with ketamine and the back of the head was shaved for access to the cisterna magna. The animal was placed in lateral recumbence and the head was tilted forward. The cisterna magna was accessed using an over-the-needle catheter and placement was verified by the presence of CSF. The animal was slowly infused with 1.5 ml of vector, followed by a flush of 0.2 ml of sterile saline. The needle was removed and the animal was allowed to recover normally. For lumbar intrathecal injections, each animal was sedated, placed on its stomach, a small skin incision made over L3–L4 and a 22-gauge spinal needle introduced into the intrathecal space using clean technique. Placement of the needle was verified by fluoroscopy. The vector (1 ml) was slowly injected by hand, the needle withdrawn and the incision site closed. Each animal was maintained in a ventral recumbancy until recovered from anesthesia. In all experiments, subjects were killed at 4 weeks post-injection and perfused with PBS. Serum samples were collected before injection and at the time of being killed. CSF samples were collected just before injection, 2 h post-injection and at the time of being killed.

At the time of killing, samples of the liver, spleen, kidney, heart, lung and testis were collected. For the intracisternal injections and intrathecal animals 303 and 304, the brain was divided into six coronal blocks (see Supplementary Figure 5) and samples from each block were sectioned at 5–7 μm on a cryostat. Sections from the cervical, thoracic and lumbar spinal cord and DRG were also collected. These sections were subjected to IHC against GFP (or with no primary antibody as a control) for gene expression analysis. Conditions were optimized so that IHC performed on naïve animal tissue showed no background staining; positive and negative control images are provided in Supplementary Figure 4. In each sample, seven random fields were selected for histomorphometric analysis of the percentage of the area that was positive for GFP, to provide an unbiased quantification of the gene expression biodistribution. For the follow-up intrathecal studies, the same samples were collected, except that the brain was divided into five coronal blocks (see Supplementary Figure 6) and the optic nerve was also collected. Brain, spinal cord, DRG, optic nerve, liver and spleen sections were collected and subjected to IHC against GFP and histomorphometric analysis on two random fields, as was done for the four animals injected into the cisterna magna. These IHC and histomorphometric studies were carried out by MPI Research. Samples from the identical regions on the contralateral side were sent to UNC for biodistribution analysis.

The above-mentioned samples stained for GFP were used for quantification of GFP-positive cells in specific brain areas. An inverted Leica DMIRB microscope with a color Micropublisher camera was used to generate the images at an objective of × 20 (Supplementary Figure 7). The number of GFP-positive brown (DAB) cells, as well as the total number of blue (cresyl violet) nuclei, were manually counted and the percentage of GFP-positive cells for each brain region was calculated.

To perform cellular identification of the GFP-transduced cells, 40 μm brain sections were incubated at 4° in PBS-T (1 × PBS + 0.1% Triton X-100) containing 3% serum and a rabbit anti-GFP (1:500; Millipore; no. AB3080), mouse anti-GFAP (1:1000; Sigma, St Louis, MO, USA; no. 032M4779) or mouse anti-NeuN (1:500; Millipore; no. MAB377). At 48 h post-incubation; these samples were washed in PBS-T and incubated with Alexa Fluor 488-conjugated goat anti-rabbit immunoglobulin G (1:2000; Invitrogen; no. A11008) and Alexa Fluor 594-conjugated goat anti-mouse immunoglobulin G (1:2000; Invitrogen; no. A11032). In all, 40 μm spinal cord sections were incubated with a rabbit anti-GFP (1:500) antibody and a goat anti-ChAT (1:1000; Millipore; no. AB144P) primary. These samples were washed and incubated with Alexa Fluor 488-conjugated donkey anti-rabbit (1:2000; Invitrogen; no. A21206) and Alexa Fluor 594-conjugated donkey anti-goat immunoglobulin G (1:2000; Invitrogen; no. A11058). Both brain and spinal cord samples were washed and mounted onto slides, visualized on a Leica SP2 confocal microscope with a × 20 objective. Each image is merged from at least five serial *Z*-stacks. Unstained brain and spinal cord sections at 40 μm were mounted onto slides for native GFP visualization.

NHP NAb titer

NHP NAb titer was determined exactly as described.[3] The NAb titer reported is the serum or CSF dilution showing a 50% decrease in the transduction of HeLa RC32 cells.

CONFLICT OF INTEREST

The authors declare no conflict of interest.

ACKNOWLEDGEMENTS

This work was supported by generous grants from Hannah's Hope Fund (to SJG), Award Number UL1RR025747 from the National Center for Research Resources (to SJG), the Senator Paul D Wellstone Muscular Dystrophy Cooperative Research Center Grant U54-AR056953 (to RJS), NIH Research Grant 5R01AI072176-05 (to RJS) and NIH Research Grant NS35633 (to TJM), as well as a kind gift from the Jasper Against Batten Foundation at Partnership for Cures (for support of SJG's research). We are extremely thankful to MPI Research for the quality and timeliness of the work and for help with study design; in particular, we would like to acknowledge the roles of Mark Johnson, Missy Peet and David Serota. We thank the UNC Vector Core, in particular Josh Grieger, for technical assistance with vector production. We also thank Lavanya Bachaboina, Huijing Sun and Erica Jones for help with tissue sectioning and IHC, Brendan Fitzpatrick and Jennifer Coleman in Mark Zylka's laboratory (UNC) for help with intrathecal mouse injections and Swati Yadav and Hung-Jui 'Sophia' Shih for running qPCR reactions. We would also like to acknowledge Jim Wilson's group at the University of Pennsylvania for the discovery of AAV9, and thank Xiao Xiao at UNC and the UNC Vector Core for providing the AAV9 helper plasmid.

REFERENCES

1 Duque S, Joussemet B, Riviere C, Marais T, Dubreil L, Douar AM *et al.* Intravenous administration of self-complementary AAV9 enables transgene delivery to adult motor neurons. *Mol Ther* 2009; **17**: 1187–1196.
2 Foust KD, Nurre E, Montgomery CL, Hernandez A, Chan CM, Kaspar BK. Intravascular AAV9 preferentially targets neonatal neurons and adult astrocytes. *Nat Biotechnol* 2009; **27**: 59–65.
3 Gray SJ, Matagne V, Bachaboina L, Yadav S, Ojeda SR, Samulski RJ. Preclinical differences of intravascular AAV9 delivery to neurons and glia: a comparative study of adult mice and nonhuman primates. *Mol Ther* 2011; **19**: 1058–1069.
4 Gray SJ, Blake BL, Criswell HE, Nicolson SC, Samulski RJ, McCown TJ *et al.* Directed evolution of a novel adeno-associated virus (AAV) vector that crosses the seizure-compromised blood–brain barrier (BBB). *Mol Ther* 2010; **18**: 570–578.
5 Samaranch L, Salegio EA, San Sebastian W, Kells AP, Foust KD, Bringas JR *et al.* Adeno-associated virus serotype 9 transduction in the central nervous system of nonhuman primates. *Hum Gene Ther* 2012; **23**: 382–389.
6 Davidson BL, Stein CS, Heth JA, Martins I, Kotin RM, Derksen TA *et al.* Recombinant adeno-associated virus type 2, 4, and 5 vectors: transduction of variant cell types and regions in the mammalian central nervous system. *Proc Natl Acad Sci USA* 2000; **97**: 3428–3432.
7 Liu G, Martins IH, Chiorini JA, Davidson BL. Adeno-associated virus type 4 (AAV4) targets ependyma and astrocytes in the subventricular zone and RMS. *Gene Therapy* 2005; **12**: 1503–1508.
8 Ghodsi A, Stein C, Derksen T, Martins I, Anderson RD, Davidson BL. Systemic hyperosmolality improves beta-glucuronidase distribution and pathology in murine MPS VII brain following intraventricular gene transfer. *Exp Neurol* 1999; **160**: 109–116.
9 Storek B, Harder NM, Banck MS, Wang C, McCarty DM, Janssen WG *et al.* Intrathecal long-term gene expression by self-complementary adeno-associated virus type 1 suitable for chronic pain studies in rats. *Mol Pain* 2006; **2**: 4.
10 Towne C, Pertin M, Beggah AT, Aebischer P, Decosterd I. Recombinant adeno-associated virus serotype 6 (rAAV2/6)-mediated gene transfer to nociceptive neurons through different routes of delivery. *Mol Pain* 2009; **5**: 52.
11 Vulchanova L, Schuster DJ, Belur LR, Riedl MS, Podetz-Pedersen KM, Kitto KF *et al.* Differential adeno-associated virus mediated gene transfer to sensory neurons following intrathecal delivery by direct lumbar puncture. *Mol Pain* 2010; **6**: 31.

12 Kao JH, Chen SL, Ma HI, Law PY, Tao PL, Loh HH. Intrathecal delivery of a mutant micro-opioid receptor activated by naloxone as a possible antinociceptive paradigm. *J Pharmacol Exp Ther* 2010; **334**: 739–745.
13 Snyder BR, Gray SJ, Quach ET, Huang JW, Leung CH, Samulski RJ *et al.* Comparison of adeno-associated viral vector serotypes for spinal cord and motor neuron gene delivery. *Hum Gene Ther* 2011; **22**: 1129–1135.
14 Storek B, Reinhardt M, Wang C, Janssen WG, Harder NM, Banck MS *et al.* Sensory neuron targeting by self-complementary AAV8 via lumbar puncture for chronic pain. *Proc Natl Acad Sci USA* 2008; **105**: 1055–1060.
15 Federici T, Taub JS, Baum GR, Gray SJ, Grieger JC, Matthews KA *et al.* Robust spinal motor neuron transduction following intrathecal delivery of AAV9 in pigs. *Gene Therapy* 2011; **19**: 852–859.
16 Gray SJ, Foti SB, Schwartz JW, Bachaboina L, Taylor-Blake B, Coleman J *et al.* Optimizing promoters for recombinant adeno-associated virus-mediated gene expression in the peripheral and central nervous system using self-complementary vectors. *Hum Gene Ther* 2011; **22**: 1143–1153.
17 Bowles DE, McPhee SW, Li C, Gray SJ, Samulski JJ, Camp AS *et al.* Phase 1 gene therapy for Duchenne muscular dystrophy using a translational optimized AAV vector. *Mol Ther* 2012; **20**: 443–455.
18 Boutin S, Monteilhet V, Veron P, Leborgne C, Benveniste O, Montus MF *et al.* Prevalence of serum IgG and neutralizing factors against adeno-associated virus (AAV) types 1, 2, 5, 6, 8, and 9 in the healthy population: implications for gene therapy using AAV vectors. *Hum Gene Ther* 2010; **21**: 704–712.
19 Swindle MM. *Swine in the Laboratory: Surgery, Anesthesia, Imaging, and Experimental Techniques*. 2nd ed (CRC Press: Boca Raton, FL, 2007; 471).
20 Morgan CJ, Pyne-Geithman GJ, Jauch EC, Shukla R, Wagner KR, Clark JF *et al.* Bilirubin as a cerebrospinal fluid marker of sentinel subarachnoid hemorrhage: a preliminary report in pigs. *J Neurosurg* 2004; **101**: 1026–1029.
21 Pardridge WM. *Transnasal and Intraventricular Delivery of Drugs. Peptide Drug Delivery to the Brain*. Raven Press: New York, 1991.
22 Pardridge WM. Drug transport in brain via the cerebrospinal fluid. *Fluids Barriers CNS* 2011; **8**: 7.
23 Snyder BR, Gray SJ, Quach ET, Huang JW, Leung CH, Samulski RJ *et al.* Comparison of adeno-associated viral vector serotypes for spinal cord and motor neuron gene delivery. *Hum Gene Ther* 2011; **22**: 1129–1135.
24 McCarty DM, Fu H, Monahan PE, Toulson CE, Naik P, Samulski RJ. Adeno-associated virus terminal repeat (TR) mutant generates self-complementary vectors to overcome the rate-limiting step to transduction in vivo. *Gene Therapy* 2003; **10**: 2112–2118.
25 McCarty DM, Monahan PE, Samulski RJ. Self-complementary recombinant adeno-associated virus (scAAV) vectors promote efficient transduction independently of DNA synthesis. *Gene Therapy* 2001; **8**: 1248–1254.
26 Xiao X, Li J, Samulski RJ. Production of high-titer recombinant adeno-associated virus vectors in the absence of helper adenovirus. *J Virol* 1998; **72**: 2224–2232.
27 Grieger JC, Choi VW, Samulski RJ. Production and characterization of adeno-associated viral vectors. *Nat Protoc* 2006; **1**: 1412–1428.
28 Paxinos G, Watson C. *The Rat Brain in Stereotaxic Coordinates*. 6th edn (Academic Press/Elsevier: Amsterdam; Boston, 2007.
29 Hylden JL, Wilcox GL. Intrathecal morphine in mice: a new technique. *Eur J Pharmacol* 1980; **67**: 313–316.
30 Sowa NA, Street SE, Vihko P, Zylka MJ. Prostatic acid phosphatase reduces thermal sensitivity and chronic pain sensitization by depleting phosphatidylinositol 4,5-bisphosphate. *J Neurosci* 2010; **30**: 10282–10293.

Supplementary Information accompanies this paper on Gene Therapy website (http://www.nature.com/gt)